DYNAMIC MASS LOSS FROM GREENLAND'S PERIPHERAL GLACIERS

by

Katherine E. Bollen

A thesis

submitted in partial fulfillment

of the requirements for the degree of

Master of Science in Geophysics

Boise State University

August 2021

BOISE STATE UNIVERSITY GRADUATE COLLEGE

DEFENSE COMMITTEE AND FINAL READING APPROVALS

of the thesis submitted by

Katherine E Bollen

Thesis Title: Dynamic Mass Loss from Greenland's Peripheral Glaciers

Date of Final Oral Examination: 28 April 2021

The following individuals read and discussed the thesis submitted by student Katherine Eleanore Bollen, and they evaluated the student's presentation and response to questions during the final oral examination. They found that the student passed the final oral examination.

Ellyn Enderlin, Ph.D.	Chair, Supervisory Committee
HP Marshall, Ph.D.	Member, Supervisory Committee
T. Dylan Mikesell, Ph.D.	Member, Supervisory Committee

The final reading approval of the thesis was granted by Ellyn Enderlin, Ph.D., Chair of the Supervisory Committee. The thesis was approved by the Graduate College.

ACKNOWLEDGMENTS

This research is funded by NASA award 80NSSC18K1228. DEMs are provided by the Polar Geospatial Center under NSF-OPP awards 1043681, 1559691, and 1542736.

Many thanks to my peers, advisor, family, and friends for their endless support during this research.

ABSTRACT

While global glacier mass balance has decreased rapidly over the last two decades, mass loss has been greatest in regions with marine-terminating glaciers. In Greenland, peripheral glaciers and ice caps (GICs) cover only ~5% of Greenland's area but contributed ~14-20% of the island's ice mass loss between 2003-2008. Although Greenland GIC's mass loss due to surface meltwater runoff have been estimated using atmospheric models, mass loss due to changes in ice discharge into surrounding ocean basins (i.e., dynamic mass loss) remains unquantified. Here, we use the flux gate method to estimate discharge from Greenland's 594 marine-terminating peripheral glaciers between 1985 – 2018, and compute dynamic mass loss as the discharge anomaly relative to the 1985-1998 period. Greenland GIC discharge averages 2.14 Gt/yr from 1985-1998 and abruptly increases to an average of 3.87 Gt/yr from 1999-2018, indicating a -1.72 Gt/yr mass anomaly. This mass loss is driven by synchronous widespread acceleration around Greenland and, like the ice sheet, is primarily caused by changes in discharge from a small number of glaciers with larger discharge. These estimates indicate that although Greenland GICs are small, they are sensitive to changes in climate and should not be overlooked in future analyses of glacier dynamics and mass loss.

TABLE OF CONTENTS

LIST OF TABLES

LIST OF FIGURES

LIST OF ABBREVIATIONS

DEM	digital elevation model
GICs	Greenland peripheral glaciers and ice caps
GLIMS	Global Land Ice Measurements from Space
GrIS	Greenland ice sheet
RACMO	Regional Atmospheric Climate Model
RGI	Randolph Glacier Inventory
SMB	surface mass balance

CHAPTER ONE: INTRODUCTION

Glacier mass loss is a major contributor to sea level rise, which impacts coastal communities globally (IPCC, 2014). The mass balance of glaciers worldwide has rapidly decreased over the last two decades (Rignot et al., 2011; Gardner et al., 2013; Zemp et al., 2019), and mass loss is generally greatest for regions with marine-terminating glaciers since these glaciers are subject to both atmospheric and oceanic forcing (Straneo et al., 2012). Although there have been tremendous advances in the understanding of marine-terminating glacier sensitivity to atmospheric and oceanic conditions over the last two decades, this sensitivity remains a critical limitation to predicting future global land ice volume and sea level rise as well as changes to ocean properties and circulation (Straneo et al., 2012; Catania et al., 2020). Mass contributions to sea level rise from the Greenland ice sheet (GrIS) have been well documented (Enderlin et al., 2014; King et al., 2018; Mankoff et al., 2020). However, there are fewer observations for Greenland's peripheral glaciers, and regional trends cannot be confidently extrapolated from the ice sheet to these glaciers (Rignot et al., 2008; van den Broeke et al., 2009).

Greenland's peripheral glaciers and ice caps (GICs; Figure 1.1) account for ~12% of global ice area outside of the Greenland and Antarctic ice sheets (Noël et al., 2017). GICs occupy only ~5% of Greenland's area but contributed ~20% (~38-41 ± 7 Gt/yr) of mass loss from Greenland's terrestrial ice masses between 2003-2008 (Bolch et al., 2013; Gardner et al., 2013). The portion of this mass loss due to the imbalance between surface accumulation and meltwater runoff, called surface mass balance (SMB), is estimated to

have steadily increased for GICs from 11.3 Gt/yr in 1997 to 36.2 Gt/yr in 2015 (Noël et al., 2017). The other component of glacier mass loss, which is the rate at which ice is discharged into the ocean due to dynamic processes (i.e., dynamic mass loss), is expected to be on the order of gigatons per year based on the difference between total mass loss and SMB. However, the large uncertainty in SMB (~15.7 Gt/yr) for GICs prevents confident partitioning of mass loss.

Here, we quantify ice discharge from Greenland's 594 marine-terminating peripheral glaciers (Figure 1.1) using the fluxgate method (Enderlin et al., 2014; King et al., 2018; Mankoff et al., 2020) and compare it to the dynamic mass loss estimates inferred from the independent total mass loss and SMB estimates. We use remotely-sensed data from satellite and airborne observations to estimate discharge as the ice flux in the direction towards glacier termini. We also provide estimates of flux corrections to account for surface accumulation and meltwater runoff between flux gates and termini using SMB estimates from the Regional Atmospheric Climate Model. Finally, we estimate temporal changes in ice thickness at the flux gates using the sparse observations of terminus position, speed, and elevation change that are presently available and provide regional estimates of near terminus rates of thickness change.

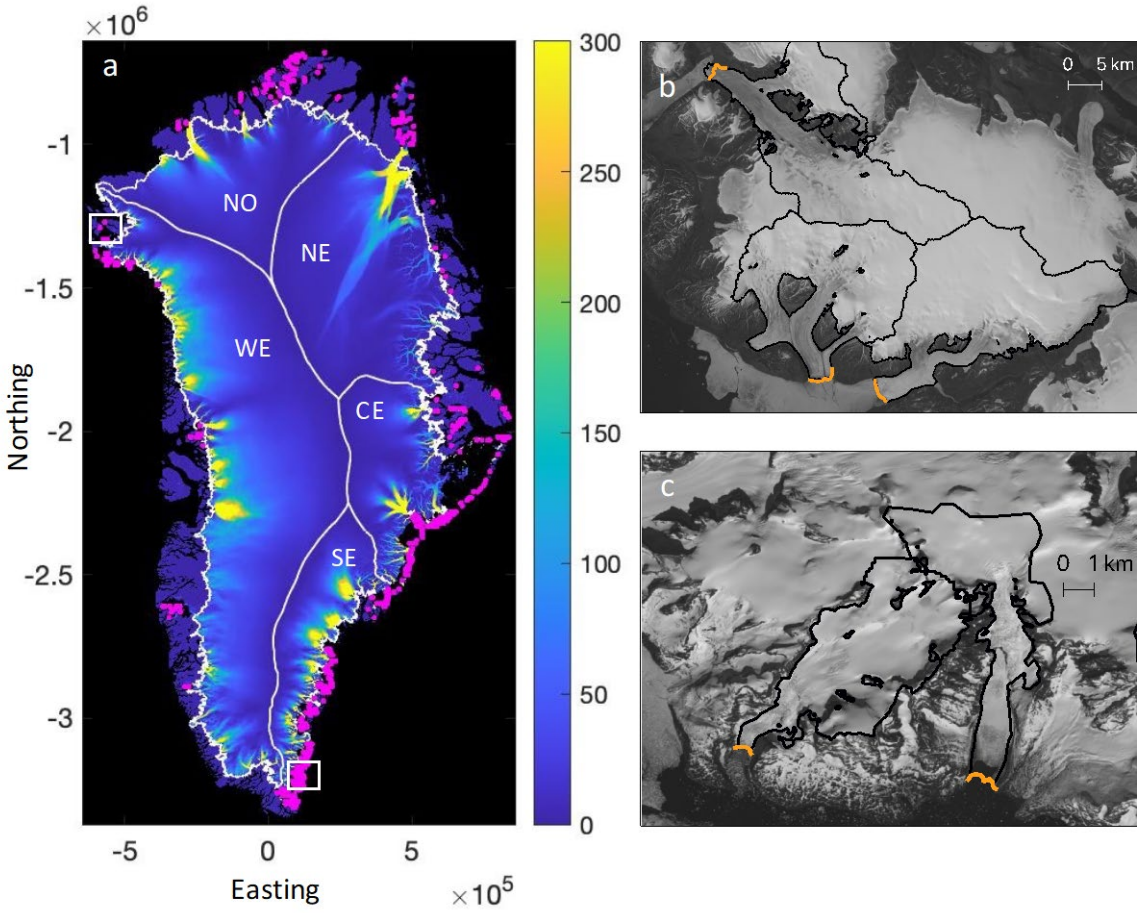

Figure 1.1 (a) The marine-terminating peripheral glaciers (pink points) overlaying the MEaSUREs velocity mosaic (m/yr) with the five regions used for this analysis. (b) Each glacier has an RGI outline (black) and a manual terminus delineation from 2000 (orange) and 2015 (red) as illustrated in the zoomed-in panels from Western and (c) Southeastern Greenland.

CHAPTER TWO: DYNAMIC MASS LOSS

2.1 Data and Methods

The Randolph Glacier Inventory (RGI) Greenland glacier outlines compiled as part of the Global Land Ice Mapping from Space program (GLIMS) are used to identify potential marine-terminating glaciers peripheral to the Greenland ice sheet. The outlines are overlain on summer Landsat 7 and 8 panchromatic images from 2000 and 2015, respectively, and terminus positions are traced to assess whether each glacier is marine-terminating and to characterize terminus position change. Based on the relatively stable terminus positions observed for the Greenland Ice Sheet's marine-terminating glaciers prior to the early 2000s (Howat and Eddy, 2011), we use the 2000 terminus delineations to characterize the steady-state terminus positions. Similarly, given that changes in ice sheet discharge have been correlated with terminus change (King et al., 2020) and that the ice sheet's discharge at least temporarily stabilized in the 2010s (Mankoff et al., 2020; King et al., 2020), we use the 2015 terminus delineations to characterize terminus positions likely following a period of retreat. A total of 641 glaciers are identified as peripheral marine-terminating glaciers using this approach. Since we are interested in discharge from only GICs, not glaciers connected to the ice sheet, we filter our dataset to exclude GrIS outlet glaciers for which Mankoff et al. (2020) calculated solid ice discharge. Although numerous GrIS discharge datasets are available, we use the Mankoff et al. (2020) dataset for filtering because it is updated regularly. There were 47

overlapping glaciers, which are excluded from our dataset, resulting in 594 glaciers used for this analysis.

Using the flux gate method, a "flux gate" perpendicular to ice flow is delineated inland of the glacier's terminus and the mass of ice that flows across the flux gate towards the terminus is used to estimate discharge. The flux gate is usually assigned near the grounding line (Enderlin et al., 2014; King et al., 2018) and can also be assigned algorithmically using a velocity mosaic and robust digital bed elevation models (Mankoff et al., 2020). However, for grounded glacier termini, the grounding line is co-located with the terminus. Since there are very few bed elevation estimates for the peripheral glaciers, however, we cannot determine whether glaciers are grounded by differencing surface and bed elevations. Therefore, we use the ArcticDEM digital elevation model (DEM; Porter et al., 2020) to identify floating termini as an observably distinct break in slope at elevations below 50 m, under the assumption that the majority of the relatively narrow and slow-flowing glaciers around Greenland's periphery will not be thicker than 500 m at their grounding lines. Only 8 glaciers are identified with potential floating termini, and the flux gates at those glaciers are set inland of the apparent floating ice. In the absence of floating ice, we position the flux gate within ~2 km of the more retracted terminus position. The flux gate is manually delineated approximately perpendicular to flow using the 250 m-resolution MEaSUREs velocity mosaic for Greenland (Joughin et al., 2016; https://nsidc.org/data/NSIDC-0670/versions/1).

The mass flux across each gate is calculated as the volume flux (i.e., product of the speed perpendicular to the gate, thickness, and width) multiplied by the depth-averaged density. Velocities are obtained from the NASA MEaSUREs ITS_LIVE project

(Gardner et al., 2019), which provides annual mean surface velocities derived from Landsat 4, 5, 7, and 8 using the auto-RIFT feature tracking processing chain described in Gardner et al. (2018). These data have 240 m-resolution and annual coverage from 1985 to 2018. To account for across-glacier variations in speed and irregular flux gate geometries, each flux gate is divided into discrete bins with widths based on the intersection of the gate with each velocity raster cell. For each bin, the speed is extracted perpendicular to the gate.

Thickness data for Greenland's peripheral glaciers are incredibly sparse. The NASA Operation Ice Bridge (OIB) mission conducted annual airborne-radar surveys across Greenland from 2009 to 2018 but focused primarily on data acquisition for the ice sheet. There are only a handful of thickness observations within a few kilometers of peripheral glacier termini and in cross-sectional orientation that can be used to constrain the geometries of Greenland's peripheral glaciers. Therefore, we use the MCoRDS L2 Ice Thickness Version 1 with 4.5 m vertical resolution, ~25 m along-track resolution, and ~14 m sample spacing (Paden et al., 2019) to devise an empirical scaling relationship with which to estimate ice thickness from width and speed observations (Enderlin et al., 2014). Only 4 of the 594 peripheral glaciers have cross-sectional OIB thickness observations at the terminus, and these glaciers are scattered between the West, Southeast, and Central-east regions. We find that for our glaciers with MCoRDS thickness data, the flux across each bin can be approximated using a second-order polynomial function ($y = 0.00068x^2 – 33.6x$) relating the flux to the product of bin speed and glacier width with an $r^2 = 0.85$ (Figure 2.1). The flux from each individual bin is multiplied by the ratio of glacier width to bin width to convert to flux across the flux gate.

For the lowest fluxes the quadratic fit is replaced with a simple linear fit ($y = 172.3x$, $r^2 = 0.66$) forced through the origin to ensure that the flux goes to zero as speed approaches zero. Beyond the upper limit of the data domain, the slope of the quadratic polynomial is held constant in order to avoid unrealistically large fluxes for the fastest-flowing glaciers. For each glacier, a flux cross-section is calculated using the empirical scaling relationships and the 1985-2018 median ITS_LIVE speed in each pixel along the cross-section. Although ideally steady-state velocities should be used to calculate ice thickness and we anticipate that dynamic change has occurred since 1985 given the rapid changes observed for nearby GrIS outlet glaciers, we use the median velocities over the entire time period because only 277 of the 594 glaciers have complete velocity time series. The flux in each bin is then divided by the bin speed and width to estimate the thickness in each bin. The histogram in Figure 2.1 indicates that this empirical relationship is mostly applied at the lower end of the curve where the confidence interval is tighter and bounds all data points used to construct the curve.

The sum of the product of the bin thickness, annual speed, and width is used to construct time series of volume flux. The volume flux is multiplied by the density of ice (917 kg/m^3) to estimate the mass flux across each flux gate. In line with analyses of GrIS mass loss and surface mass balance losses for Greenland's peripheral glaciers, we compute dynamic mass loss as the discharge anomaly relative to the 1985-1998 time period. The data are clustered by region based on the regional boundaries designated by Mouginot et al. (2019) for the GrIS, with the north, central, and south west regions merged into one western region since there are so few GICs along Greenland's west coast.

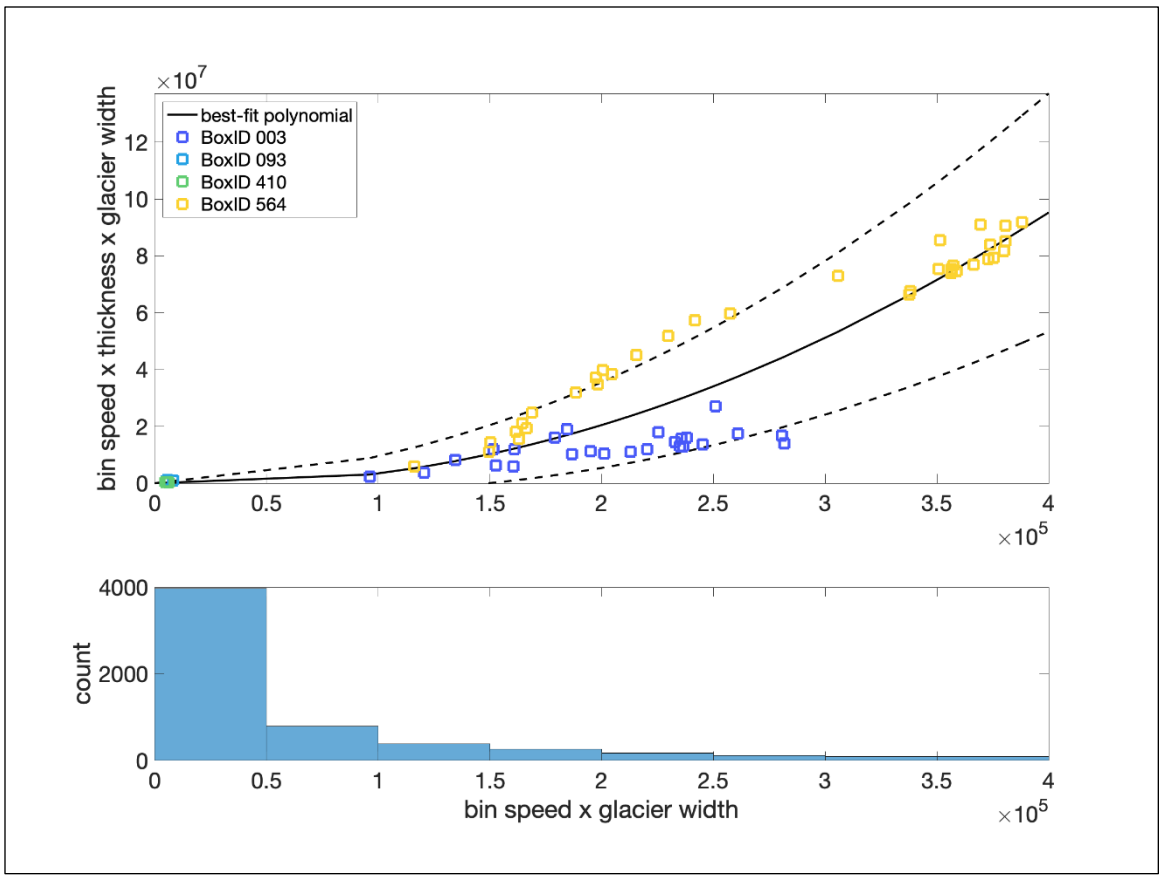

Figure 2.1 Top panel: flux calculated as the product of the bin thickness (m) and speed (m/yr) and the glacier width (m) plotted against the product of the bin speed and glacier width for the four peripheral glaciers with radar observations of cross-flow ice thickness. The solid line is the best-fit quadratic polynomial for the product of the bin speed and width greater than 1x10^5 m^2/yr and the linear polynomial forced through the origin at smaller values. The dashed lines represent the boundaries of the two sigmas (i.e., ±2 standard deviation) confidence interval. Bottom panel: the histogram illustrates the distribution of glaciers across the curve.

2.2 Dynamic Mass Loss Uncertainties

There are several sources of uncertainty in our dynamic mass loss estimates. Uncertainties in speed are extracted from the ITS_LIVE data product. Uncertainties in width are assumed to be one 15 m-resolution Landsat pixel at each end of the flux gate. We quantify uncertainty in our ice thickness estimates due to the use of the empirical scaling relationship from the confidence intervals of the polynomial fits. These

uncertainties are combined using standard error propagation techniques to constrain their influence on our flux estimates.

The use of a constant thickness cross-section for all flux calculations potentially introduces a time-varying bias into our flux time series. Although DEM time series produced by the Polar Geospatial Center ArcticDEM project are available for all glaciers, the limited and highly variable temporal coverage of the DEMs prevents the direct use of these data to constrain changes in ice thickness over the 1985-2018 time period. The number of DEMs per glacier ranges from 1-61 with an average of 11. The average time span covered by these DEMs at a given glacier is 4.3 years, and the DEMs are from any time between 2011 and 2019. In order to provide first-order estimates of temporal changes in thickness on our flux time series, we fit linear polynomials to the surface elevation time series from the DEMs available for each glacier. We also fit linear polynomials to the surface elevation data and the speed and surface mass balance from the closest observation dates in an effort to identify the most predictive relationship to extrapolate thickness changes over time.

The use of inland fluxes to approximate terminus discharge also introduces uncertainty into our dynamic mass loss estimates. We use annual SMB estimates to approximate surface mass loss or gain over the time it takes for the ice to advect from the flux gate to the terminus. The distance between the flux gate and the terminus is estimated using the 2000 terminus position for 1985-2000, the mean of the 2000 and 2015 terminus positions for 2001-2014, and the 2015 terminus position for 2015-2018. The annual ITS_LIVE speeds are used to convert the distance to an advection time. The annual 1 km-resolution Regional Atmospheric Climate Model (RACMO) SMB over the

advection time period is summed to estimate mass loss between the flux gate and terminus.

Our assumptions that surface speeds are equal to the depth-averaged speeds and that the glacier density is equal to bubble-free ice may also introduce bias into our flux estimates. However, we expect that the errors introduced by these assumptions will remain relatively constant over time and should have minimal influence on dynamic mass loss estimates.

CHAPTER THREE: DISCHARGE TIME SERIES

3.1 Results

The sum of the time-averaged glacier discharge across the GICs is 2.14 Gt/yr with a median absolute deviation (MAD) of ± $7x10^{-5}$ Gt/yr from 1985 to 1998 which we refer to as 'steady state' since this is the part of the record before the mass anomaly emerges (Figure 3.1). From 1999-2018, the sum of time-averaged glacier discharge is 3.87 ± $3x10^{-4}$ Gt/yr (Figure 3.1). 98% of the glaciers discharge less than 0.05 Gt/yr, and there are 13 glaciers, 2% of the total, that discharge more than 0.05 Gt/yr (Figure 3.2). These 13 glaciers account for 1.34 Gt/yr (63%) of the GICs discharge during the steady-state period before 1998 and 1.94 Gt/yr (50%) of the discharge after 1999. There are 277 glaciers that have complete time series which exhibit a 0.31 Gt/yr increase in discharge from an annual average of 1.56 Gt/yr before 1998 to an annual average of 1.87 Gt/yr after 1999. 57% of glaciers have velocity data from 1985 – 1998, and 93% of glaciers have velocity data from 1999 – 2018. The greatest discharge comes from the southeast and central-east regions both during the steady-state period (0.65 Gt/yr, 0.97 Gt/yr, respectively) and the 1999 – 2018 period (1.76 Gt/yr, 1.07 Gt/yr respectively, Table 3.1).

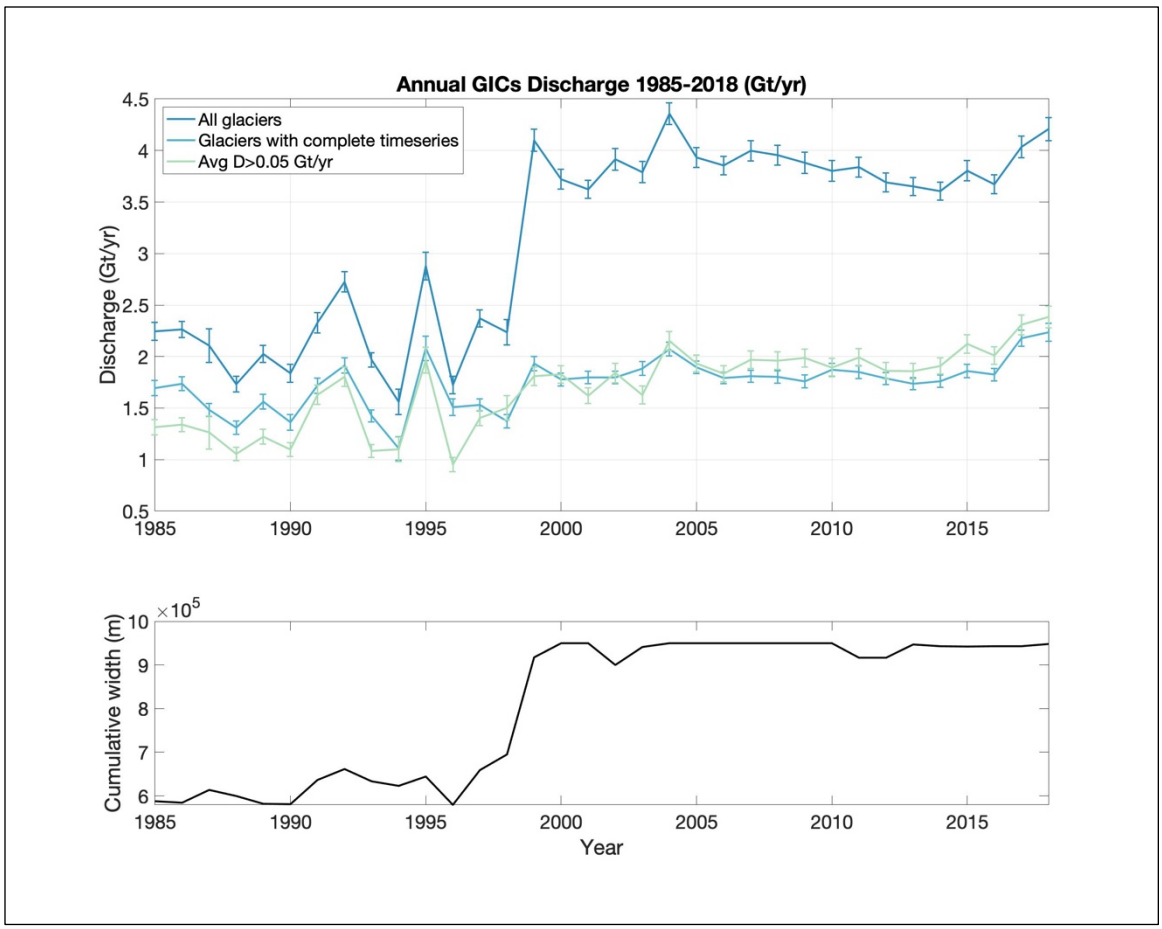

Figure 3.1 Top panel: annual discharge from the marine-terminating GICs from 1985 to 2018 (dark blue), discharge from only glaciers with complete data coverage across the time series (light blue), and discharge from glaciers with average annual discharge greater than 0.05 Gt/yr (green). Bottom panel: cumulative width of all glaciers used to calculate discharge each year.

Bolch et al. (2013) and Gardner et al. (2013) estimated the total mass budget for Greenland GICs at -38 ± 7 Gt/yr for 2003-2009 using surface elevation change observations from ICESat. Noël et al. (2017) estimated that changes in surface mass balance from 1997-2015 accounted for approximately 36.2 ± 15.7 Gt/yr of that mass loss, implying that recent dynamic mass loss should be approximately 2 Gt/yr. Under the assumption that the 1985-1998 discharge represents steady-state conditions, our discharge estimates suggest a time-averaged 1.72 Gt/yr dynamic mass loss from 1999-2018 (Figure 3.1). The jump in discharge in 1999 is present in both the total GIC

discharge time series as well as the time series for only glaciers with data across the entire record, suggesting that the sharp increase is at least in part a real signal rather than solely a sudden increase in data availability due to the launch of Landsat 7.

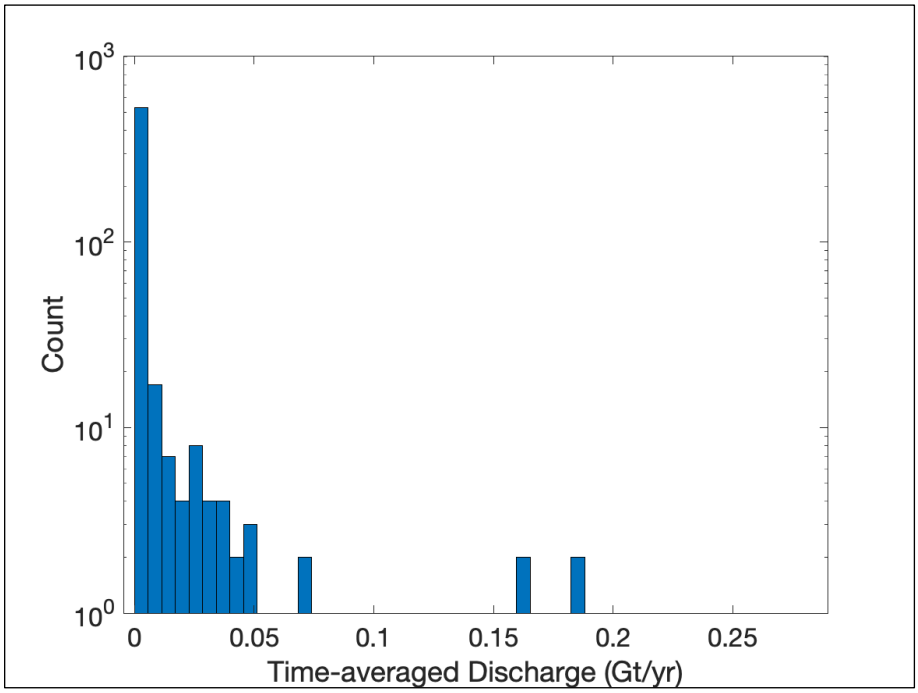

Figure 3.2 Histogram of the distribution of the time-averaged annual glacier discharge.

3.2 Thickness Change

Negative rates of thickness change dominated all regions, indicating that thinning was prevalent over the 2011-2019 time period. The regional median rate of thickness change ranged from -0.23 ± 0.85 m/yr in the north to -1.39 ± 0.27 m/yr in the central-east (Table 3.2). The small thinning rate (61.33%, Table 3.2) and large variability in the north indicates that although thinning dominates in this region, thickening is fairly common as well. The median rate of thickness change for all GICs was -0.94 ± 1.14 m/yr (Table 3.2). Overall, the correlation between thickness change and time ($r^2 = 0.20$), speed ($r^2 = 0.11$) or SMB ($r^2 = 0.10$) for the GICs is very low, indicating that changes in ice thickness

cannot be confidently extrapolated as a linear function of any of the tested variables (Table 3.2). For all but the north region, change in thickness is best, although weakly, approximated as a linear function of time. For the north, changes in thickness over time are most strongly correlated with changes in SMB.

The change in mass between the flux gate and the terminus due to surface accumulation and ablation as the ice flows from the flux gate to the terminus for all GICs is -0.33 Gt/yr during the 1985-1998 steady-state period and -0.31 Gt/yr during 1999-2018 period. In other words, our Greenland GIC discharge estimates should be lowered by ~0.32 Gt/yr to account for mass loss between the flux gates and glacier termini. These losses are equivalent to 15% of the discharge before 1998 and 8% after 1999.

Table 3.1 Regional sum of time-averaged annual glacier discharge from 1985-1998 ("steady-state") and 1999-2018, and the sum of the time-averaged SMB between the flux gate and terminus.

Region	**Discharge: 1985-1998 (Gt/yr) ± MAD**	**Discharge: 1999-2018 (Gt/yr) ± MAD**	**SMB adjustment: 1985-1998 (Gt/yr) ± MAD**	**SMB adjustment: 1999-2018 (Gt/yr) ± MAD**
North	0.02 ± 0	0.03 ± 0	0 ± 0	-0.01 ± 0
West	$0.16 \pm 8\text{x}10^{-5}$	$0.63 \pm 2\text{x}10^{-4}$	$-0.04 \pm 1\text{x}10^{-4}$	$-0.06 \pm 2\text{x}10^{-4}$
Southeast	$0.65 \pm 2\text{x}10^{-2}$	$1.76 \pm 5\text{x}10^{-4}$	$-0.07 \pm 2\text{x}10^{-5}$	$-0.12 \pm 2\text{x}10^{-4}$
Central-east	$0.97 \pm 2\text{x}10^{-4}$	$1.07 \pm 2\text{x}10^{-4}$	$-0.19 \pm 2\text{x}10^{-4}$	$-0.09 \pm 8\text{x}10^{-5}$
Northeast	$0.35 \pm 7\text{x}10^{-5}$	$0.39 \pm 1\text{x}10^{-4}$	$-0.03 \pm 4\text{x}10^{-5}$	$-0.02 \pm 5\text{x}10^{-5}$
Total	$2.14 \pm 7\text{x}10^{-5}$	$3.87 \pm 3\text{x}10^{-4}$	$-0.33 \pm 4\text{x}10^{-5}$	$-0.31 \pm 9\text{x}10^{-5}$

Table 3.2 Regional median time-averaged thickness change (ΔH), median absolute deviation (MAD) of thickness change, and median time-averaged correlation coefficients for linear polynomials used to describe thickness change as a function of time, speed, and SMB across each region.

Region	Δ H (m/yr)	Δ H MAD (m/yr)	% glaciers thinning	Time series r2	Speed r2	SMB r2
North	-0.23	0.85	61.33	0.09	0.04	0.12
West	-1.04	1.22	64.52	0.15	0.06	0.04
Southeast	-0.94	1.40	66.67	0.19	0.10	0.10
Central-east	-1.39	0.27	72.88	0.33	0.18	0.14
Northeast	-0.89	0.13	59.18	0.16	0.11	0.05
Total	-0.94	1.14	67.00	0.20	0.11	0.10

CHAPTER FOUR: TRENDS IN GICs DYNAMIC MASS LOSS

4.1 Dynamic Drivers of Mass Loss

Discharge varies spatially with glacier geometry and speed. The fastest speeds should be observed for glaciers that are wide, thick, and occupy troughs that are hundreds of meters below sea level since these conditions require fast speeds in order to maintain a balance of driving and resistive stresses (Cuffey and Paterson, 2010). Here we make use of the expected, and observed (Figure 2.1), relationships between glacier geometry and speed to estimate ice thickness. Since thickness is estimated as a piecewise function of the product of speed and glacier width that includes a non-linear component, spatial variations in discharge are not identical to patterns in speed (Figure 4.1). However, *temporal* variations in discharge are entirely dictated by changes in speed over time. We observe a sudden acceleration in 1999 in all regions except the north, which drives the step-increase in discharge in Figure 3.1. We find discharge was relatively steady before and after the 1999 step increase, with MADs of $7x10^{-5}$ Gt/yr and $3x10^{-4}$ Gt/yr for all GICs from 1985-1998 and 1999-2018, respectively. The median speeds for each region remain fairly steady from 2000-2011 after the 1999 step-increase (Figure 4.2) before dropping again in 2014-2015. The discrepancy between temporal patterns in median speed and GIC discharge reflects changes in the prevalence of glaciers with anomalously high speeds after 2012, particularly in the southeast (Figure 4.2). The time series also shows that, similar to the ice sheet, where 15 glaciers drive >50% of the discharge change (Enderlin et al., 2014), the largest glaciers (n=13) account for 50-68% of the discharge.

Thinning is prevalent across all regions (Table 3.2). Change in thickness across the GICs is most highly correlated to linear change in time ($r^2 = 0.20$, Table 3.2). However, the principle of mass conservation requires that changes in thickness over time are caused by changes in SMB, speed, or both. We attribute the overall poor correlations to the sparse data coverage and lack of temporal synchronicity between these datasets. Further, the relative importance of these drivers varies widely between glaciers based on their local climate and geometry, so linear extrapolation may be too simple. For example, Moon et al. (2012) found regional variability in speed at GrIS outlet glaciers and a variable and complex response to regional and local forcing. Given our inability to confidently extrapolate changes in thickness beyond the sparse observational records for each glacier, we do not attempt to correct our discharge estimates for temporal variations in ice thickness. The median of the change in thickness as a fraction of the total thickness observed for each glacier during the 2011-2019 period is -0.13. Assuming that the observed thinning rates can be reasonably extrapolated over the entire 1999-2018 post-acceleration time period, then our discharge estimates could be ~10-20% higher immediately following the 1999 acceleration and gradually decreasing to ~10-20% lower by 2018. However, there is no observational thickness data concurrent with the 1999 acceleration, when we would expect the largest dynamic changes in thickness to occur.

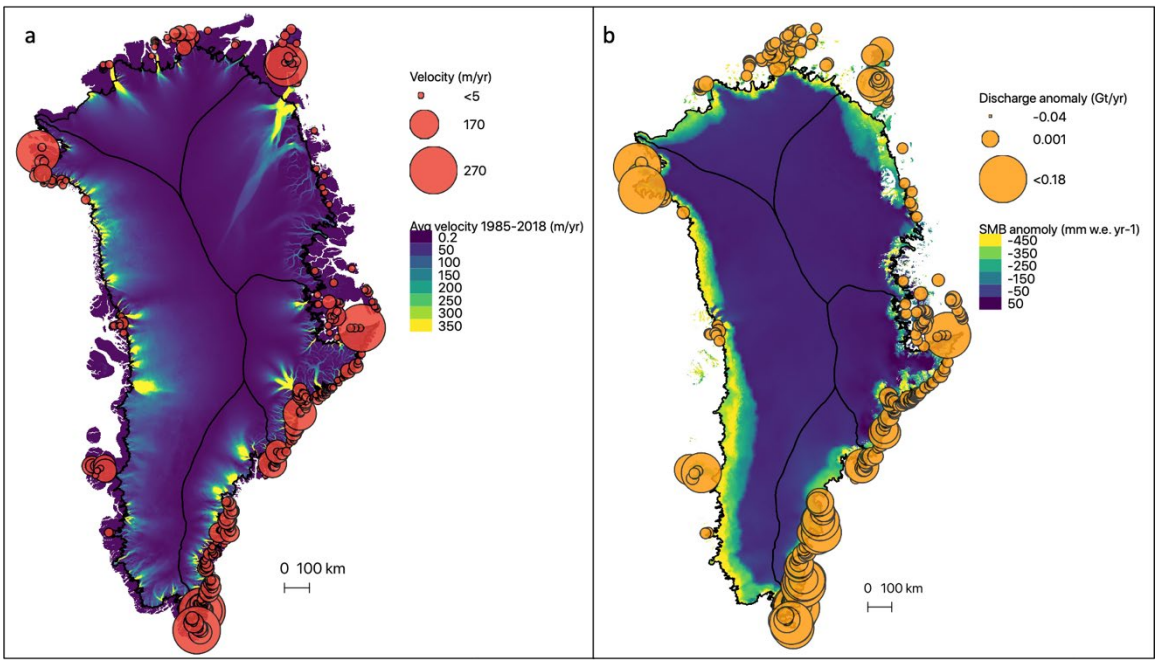

Figure 4.1 (a) Average annual velocity and (b) average annual discharge anomaly at each glacier is denoted by the size of the bubble. The background images are the MEaSUREs velocity mosaic (m/yr) and the time-averaged surface mass balance anomaly for 1999-2019 relative to the 1958-1998 steady-state conditions.

4.2 Comparison to GrIS Trends and Additional Drivers of Mass Loss

Atmospheric and oceanic forcing have been shown to drive mass loss at GrIS outlet glaciers. GrIS outlet glacier discharge was steady for ~30 years prior to 2000 (~430 Gt/yr), before it increased to >500 Gt/yr between 2000 and 2005 then temporarily stabilized at ~500 Gt/yr through present (Mankoff et al., 2020). Terminus positions were also fairly steady until the late 1990s, and retreat has been widespread throughout the early 2000s (Howat and Eddy, 2011). The onset of retreat of GrIS outlet glaciers coincided with mean air temperature increases at coastal weather stations (Moon and Joughin, 2008) and a sudden increase in subsurface ocean temperature along the west coast of Greenland (Holland et al., 2008). Greenland's GICs are less studied, but Noël et al. (2017) found 1997 ± 5 years to be a tipping point for GIC surface mass balance, as it

marked the onset of rapid deterioration in the capacity of the GICs firn to refreeze meltwater. An increase in meltwater percolation to the glacier base could potentially trigger the widespread acceleration and increased discharge observed here, although the response of glaciers to changes in meltwater are highly variable (Moon et al., 2014, Moon et al., 2012). The increase in surface meltwater production and percolation as well as changes in ocean temperatures could have also triggered terminus retreat, such as observed for GrIS outlet glaciers, driving acceleration. The decreased spatial, spectral, radiometric, and temporal resolution of the optical satellite image record prior to the launch of Landsat 7 in 1999, however, limits our ability to accurately map changes in terminus position over time. Therefore, although we present the first estimates of Greenland GIC discharge and dynamic mass loss here, we cannot confidently tease-out the processes that drove the sudden increase in discharge in 1999 and the sustained period of dynamic mass loss that ensued.

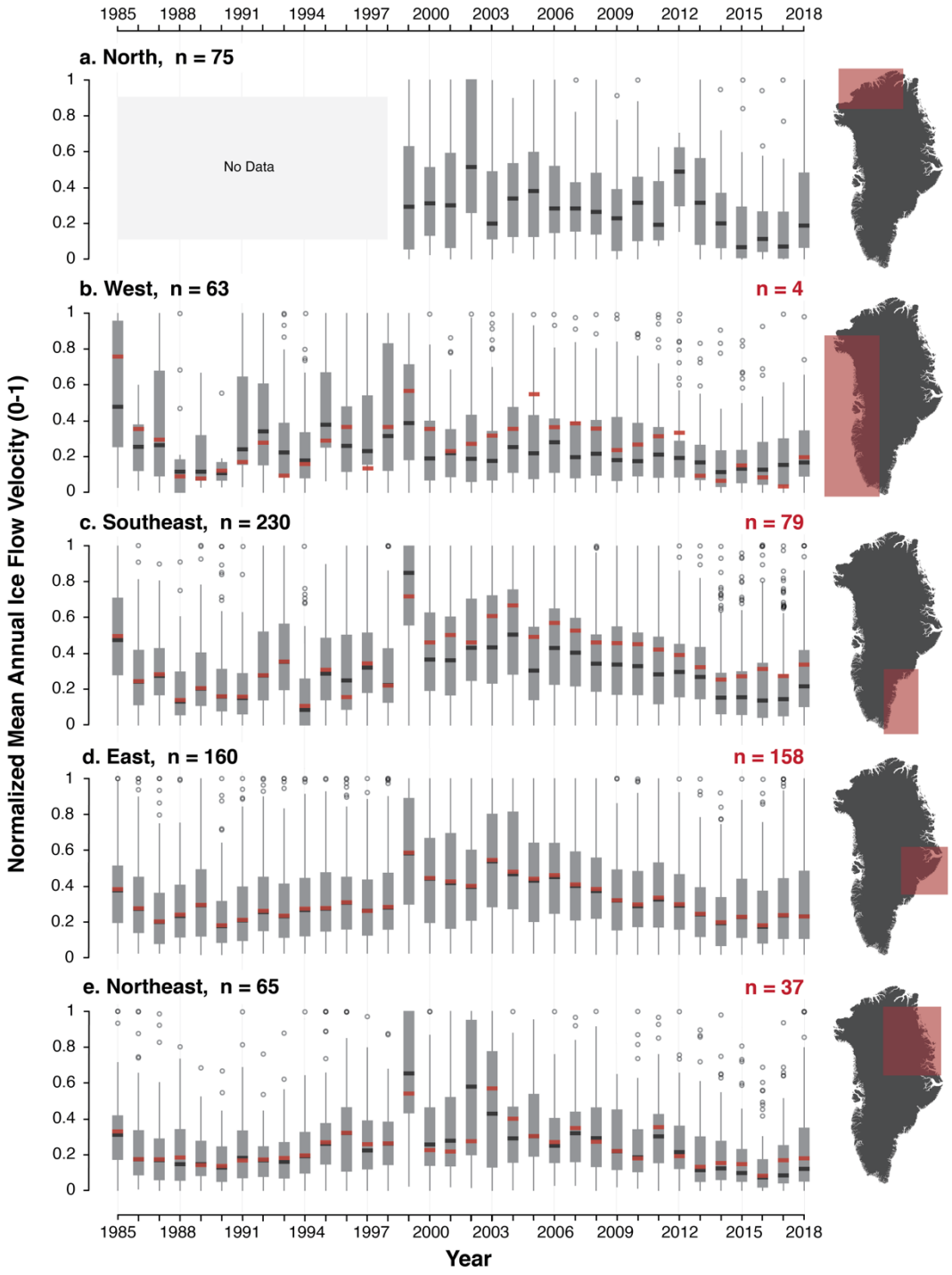

Figure 4.2 Normalized velocity by region from 1985 – 2018. The black line shows the median for all glaciers, and the red line indicates the median for only glaciers with complete records. Figure by Rebecca Muhlheim.

4.3 Conclusion and Future Work

Although GICs only cover 5% of Greenland's area, they play a substantial role in Greenland's contributions to sea level rise and freshwater flux which impact communities globally, as well as marine ecosystems and circulation. The 594 marine-terminating GICs discharged an average of 2.14 Gt/yr from 1985 to 1998, and an average of 3.87 Gt/yr between 1999 and 2018. These estimates indicate a mass anomaly of -1.72 Gt/yr which is consistent with previous mass budget estimates for these glaciers. This mass loss is driven by synchronous acceleration across the GICs, resulting in the step-increase in discharge in 1999. The cumulative discharge is driven by the 13 glaciers with the highest rate of discharge, which account for 63% of the total discharge before 1998 and 50% after 1999. Further analysis of the velocity and SMB time series is required to understand controls on thickness change at the terminus, and a comprehensive look at oceanic and atmospheric forcing will illuminate the drivers of the dynamic mass loss evident in our time series. Finally, these discharge estimates can be compared to terminus position change time series in order to estimate the intra-annual timing of mass loss and frontal ablation.

REFERENCES

Bolch, T., Sandberg Sørensen, L., Simonsen, S. B., Mölg, N., Machguth, H., Rastner, P., & Paul, F. (2013). Mass loss of Greenland's glaciers and ice caps 2003–2008 revealed from ICESat laser altimetry data. *Geophysical Research Letters*, *40*(5), 875-881.

Catania, G. A., Stearns, L. A., Moon, T. A., Enderlin, E. M., & Jackson, R. H. (2020). Future evolution of Greenland's marine-terminating outlet glaciers. *Journal of Geophysical Research: Earth Surface*, *125*(2), e2018JF004873.

Cuffey, K. M., & Paterson, W. S. B. (2010). *The physics of glaciers*. Academic Press.

Enderlin, E. M., Howat, I. M., Jeong, S., Noh, M. J., van Angelen, J. H., & van den Broeke, M. R. (2014). An improved mass budget for the Greenland ice sheet. *Geophysical Research Letters*, *41*(3), 866-872.

Gardner, A. S., M. A. Fahnestock, and T. A. Scambos, 2019: ITS_LIVE Regional Glacier and Ice Sheet Surface Velocities. Data archived at National Snow and Ice Data Center; doi:10.5067/6II6VW8LLWJ7.

Gardner, A. S., G. Moholdt, T. Scambos, M. Fahnstock, S. Ligtenberg, M. van den Broeke, and J. Nilsson, 2018: Increased West Antarctic and unchanged East Antarctic ice discharge over the last 7 years, Cryosphere, 12(2): 521–547, doi:10.5194/tc-12-521-2018.

Gardner, A. S., Moholdt, G., Cogley, J. G., Wouters, B., Arendt, A. A., Wahr, J., ... & Ligtenberg, S. R. (2013). A reconciled estimate of glacier contributions to sea level rise: 2003 to 2009. *science*, *340*(6134), 852-857.

Holland, D. M., Thomas, R. H., De Young, B., Ribergaard, M. H., & Lyberth, B. (2008). Acceleration of Jakobshavn Isbræ triggered by warm subsurface ocean waters. *Nature geoscience*, *1*(10), 659-664.

Howat, I. M., & Eddy, A. (2011). Multi-decadal retreat of Greenland's marine-terminating glaciers. *Journal of Glaciology*, *57*(203), 389-396.

IPCC, C. C. (2014). Mitigation of climate change. *Contribution of working group III to the fifth assessment report of the intergovernmental panel on climate change*.

Joughin, I., B. Smith, I. Howat, and T. Scambos. (2016). *MEaSUREs Multi-year Greenland Ice Sheet Velocity Mosaic, Version 1*, used all subsets. Boulder, Colorado USA. NASA National Snow and Ice Data Center Distributed Active Archive Center. doi: https://doi.org/10.5067/QUA5Q9SVMSJG, 2020.

Khalil, A., Grant, J. L., Caddle, L. B., Atzema, E., Mills, K. D., & Arnéodo, A. (2007). Chromosome territories have a highly nonspherical morphology and nonrandom positioning. *Chromosome research*, *15*(7), 899-916.

King, M.D., Howat, I.M., Candela, S.G. *et al.* (2020). Dynamic ice loss from the Greenland Ice Sheet driven by sustained glacier retreat. *Commun Earth Environ* **1,** 1.

King, M. D., Howat, I. M., Jeong, S., Noh, M. J., Wouters, B., Noël, B., & van den Broeke, M. R. (2018). Seasonal to decadal variability in ice discharge from the Greenland Ice Sheet. *The cryosphere*, *12*(12), 3813.

Mankoff, K. D., Solgaard, A., Colgan, W., Ahlstrøm, A. P., Khan, S. A., & Fausto, R. S. (2020). Greenland Ice Sheet solid ice discharge from 1986 through March 2020. *Earth System Science Data*, *12*(2), 1367-1383.

Moon, T., & Joughin, I. (2008). Changes in ice front position on Greenland's outlet glaciers from 1992 to 2007. *Journal of Geophysical Research: Earth Surface*, *113*(F2).

Moon, T., Joughin, I., Smith, B., & Howat, I. (2012). 21st-century evolution of Greenland outlet glacier velocities. *Science*, *336*(6081), 576-578.

Moon, T., Joughin, I., Smith, B., Van Den Broeke, M. R., Van De Berg, W. J., Noël, B., & Usher, M. (2014). Distinct patterns of seasonal Greenland glacier velocity. *Geophysical research letters*, *41*(20), 7209-7216.

Mouginot, J., Rignot, E., Bjørk, A. A., Van den Broeke, M., Millan, R., Morlighem, M., ... & Wood, M. (2019). Forty-six years of Greenland Ice Sheet mass balance from 1972 to 2018. *Proceedings of the National Academy of Sciences*, *116*(19), 9239-9244.

Noël, B., van De Berg, W. J., Lhermitte, S., Wouters, B., Machguth, H., Howat, I., ... & van den Broeke, M. R. (2017). A tipping point in refreezing accelerates mass loss of Greenland's glaciers and ice caps. *Nature Communications*, *8*(1), 1-8.

Paden, J., J. Li, C. Leuschen, F. Rodriguez-Morales, and R. Hale. (2010, updated 2019). *IceBridge MCoRDS L2 Ice Thickness, Version 1*, used all subsets. Boulder, Colorado USA. NASA National Snow and Ice Data Center Distributed Active Archive Center. doi: https://doi.org/10.5067/GDQ0CUCVTE2Q, 2019.

Porter, Claire; Morin, Paul; Howat, Ian; Noh, Myoung-Jon; Bates, Brian; Peterman, Kenneth; Keesey, Scott; Schlenk, Matthew; Gardiner, Judith; Tomko, Karen; Willis, Michael; Kelleher, Cole; Cloutier, Michael; Husby, Eric; Foga, Steven; Nakamura, Hitomi; Platson, Melisa; Wethington, Michael, Jr.; Williamson, Cathleen; Bauer, Gregory; Enos, Jeremy; Arnold, Galen; Kramer, William; Becker, Peter; Doshi, Abhijit; D'Souza, Cristelle; Cummens, Pat; Laurier, Fabien; Bojesen, Mikkel, 2018, "ArcticDEM", *https://doi.org/10.7910/DVN/OHHUKH*, Harvard Dataverse, V1, [2020].

Rignot, E., Box, J. E., Burgess, E., & Hanna, E. (2008). Mass balance of the Greenland ice sheet from 1958 to 2007. *Geophysical Research Letters*, *35*(20).

Rignot, E., Velicogna, I., van den Broeke, M. R., Monaghan, A., & Lenaerts, J. T. (2011). Acceleration of the contribution of the Greenland and Antarctic ice sheets to sea level rise. *Geophysical Research Letters*, *38*(5).

Straneo, F., et al. "Understanding the dynamic response of Greenland's marine terminating glaciers to oceanic and atmospheric forcing: a white paper by the US CLIVAR working group on Greenland Ice Sheet–Ocean Interactions (GRISO)." *US CLIVAR Office, Washington, DC* 20006 (2012): 22.

van den Broeke, M., Bamber, J., Ettema, J., Rignot, E., Schrama, E., van de Berg, W. J., ... & Wouters, B. (2009). Partitioning recent Greenland mass loss. *science*, *326*(5955), 984-986.

Zemp, M., Huss, M., Thibert, E., Eckert, N., McNabb, R., Huber, J., ... & Thomson, L. (2019). Global glacier mass changes and their contributions to sea-level rise from 1961 to 2016. *Nature*, *568*(7752), 382.